

To appear in *The Astrophysical Journal*

POWER SPECTRA OF X-RAY BINARIES

T. P. Li^{1,2,3} and Y. Muraki³

ABSTRACT

The interpretation of Fourier spectra in the time domain is critically examined. Power density spectra defined and calculated in the time domain are compared with Fourier spectra in the frequency domain for three different types of variability: periodic signals, Markov processes and random shots. The power density spectra for a sample of neutron stars and black hole binaries are analyzed in both the time and the frequency domains. For broadband noise, the two kinds of power spectrum in accreting neutron stars are usually consistent with each other, but the time domain power spectra for black hole candidates are significantly higher than corresponding Fourier spectra in the high frequency range (10–1000 Hz). Comparing the two kinds of power density spectra may help to probe the intrinsic nature of timing phenomena in compact objects.

Subject headings: Stars: binaries — Stars: neutron — X-rays: stars — Methods: data analysis

1. INTRODUCTION

The Fourier transform is widely used in timing analysis in astronomy. Through a discrete Fourier transform, a light curve $x(t_k)$ can be decomposed into sine wave components in the frequency domain

$$a(f_j) = \sum_k x(t_k) e^{-i2\pi f_j k \Delta t} , \quad (1)$$

¹Department of Physics & Center for Astrophysics, Tsinghua University, Beijing

²Institute of High Energy Physics, Chinese Academy of Sciences, Beijing

³Solar-Terrestrial Environment Laboratory, Nagoya University, Nagoya

where $a(f_j)$, $j = -N/2, \dots, N/2 - 1$, is the Fourier amplitude of sine wave components at frequency $f_j = j\Delta f$ with $\Delta f = 1/(N\Delta t)$ and $x(t_k)$ represents the photon counts during a time interval $(t_k, t_k + \Delta t)$, $k = 1, 2, \dots, N$, with $t_k = (k - 1)\Delta t$. The Fourier spectrum can be a powerful technique in the search for periodic signals, pulsations, and quasi-periodic oscillations in the light curve of a X-ray source. The Fourier power density

$$p_f(f_j) = |a(f_j)|^2 \quad (2)$$

is used to describe the variability amplitude at different frequency f_j . A peak with power in excess of the noise distribution power in the Fourier spectrum indicates the existence of a periodic component in the light curve. When estimating the amplitude of a periodic signal from the Fourier power density spectrum, one must assume that the shape of a signal pulse is sinusoidal, which is usually not true for variability due to real physical processes.

Even more care should be taken in interpreting the Fourier spectrum of an aperiodic process in the time domain. It is a prevalent misconception that the Fourier power spectrum is the only way to express the distribution of variability amplitude vs. time scale, and that $p_f(f_j)$ is a quantity describing the variability amplitude for the time scale $1/f_j$. The actual relation between the Fourier power and the variability process occurring in the time domain is given by Parseval's theorem:

$$\frac{1}{N} \sum_{j=-N/2}^{N/2-1} |a(f_j)|^2 = \sum_{k=1}^N |x(t_k)|^2, \quad (3)$$

or equivalently,

$$\sum_j p_f(f_j) \Delta f = \sum_k |r(t_k)|^2 \Delta t, \quad (4)$$

where $r(t_k) = x(t_k)/\Delta t$ is the counting rate at t_k . Parseval's theorem states that the integral of the Fourier power density over the whole frequency range is equal to the variability power of the same process in the time domain. In fact, that is just the reason why the quantity $p_f(f_j) = |a(f_j)|^2$ is called *power density*. However, Parseval's theorem says nothing about the power density *distribution* over the time domain. The Fourier power at any given frequency within the limited range, $0 \rightarrow 1/\Delta t$, actually represents a sum of complex amplitudes from an infinite number of aliased frequencies, each contribution of which is reduced by a factor of $\text{sinc}(\pi f \Delta t)$, with the sum of the squares of all the factors being unity. In contrast, the power at any given frequency in a time-based spectrum is most sensitive to the *rate of change* of the Fourier spectrum with frequency near the Nyquist frequency ($f = 1/(2\Delta t)$) and its aliases, since the sinc function given above is changing most rapidly for such frequencies. The rms variation vs. time scale of a time series may, in fact, differ substantially from its Fourier spectrum. Even in the simplest case, where the

signal is purely sinusoidal with a frequency f , the Fourier spectrum is a δ function for the continuous Fourier transform or approximately a δ function for the discrete case. Such a function has little power density at frequencies except those near f , which, although in this case is a clear representation of what physical process is going on, is still not an accurate representation of the variability of the amplitude in a time series. Only when the time step is set equal to or much greater than the period, $\Delta t \geq 1/f$, can the corresponding light curve (or pulse profile) of a sinusoidal signal be completely flattened to make the time variation vanish. At time scales shorter than $1/f$, however, a variation of intensity still exists in the light curve, and under some circumstances one would wish that power over this region should not be zero. In fact, different but mathematically equivalent representations with different bases or functional coordinates in the frequency domain do exist for certain light curves. The Fourier transform with its trigonometric basis is just one of many possible transforms between the time and frequency domains, and may not necessarily represent the true power distribution of a *physical* process in the time domain.

One can also argue that any observable physical process always occurs in the time domain, and this is why real variability amplitudes at different time scales are useful in understanding a time varying process, in addition to the understanding gleaned from the conventional Fourier spectrum. An algorithm to calculate the power density spectrum directly in the time domain without using the Fourier transform has been proposed (Li 2001). We introduce the algorithm and compare the power spectra in the time domain with the Fourier spectra for different kinds of time process model in §1. We have studied the power density spectra of a sample of neutron stars and black hole binaries, in both the frequency *and* the time domains. The results are presented in §3. A discussion of the potential gain in the understanding the intrinsic nature of physical processes occurring near compact objects via comparison of the two kinds of power density spectrum is given in §4.

2. POWER SPECTRA IN THE TIME DOMAIN

The initial definition of the variation power in a light curve $x(k)$ is

$$P(\Delta t) = \frac{\text{Var}(x)}{(\Delta t)^2} = \frac{\frac{1}{N} \sum_{k=1}^N (x(k) - \bar{x})^2}{(\Delta t)^2} = \frac{1}{N} \sum_{k=1}^N (r(k) - \bar{r})^2, \quad (5)$$

where the light curve $x(k)$, $k = 1, \dots, N$, is a counting series obtained from a time history of observed photons with a time step Δt , $r(k)$ is the corresponding rate series, and $\bar{x} = \sum_{k=1}^N x(k)/N$ and $\bar{r} = \sum_{k=1}^N r(k)/N$ are the average counts and count rates, respectively. The unit used for a power P in spectral analysis in astronomy is usually rms^2 , where ‘rms’ refers to the analysed time series x . In the case of x being a counting series, the power P

can be expressed in units of counts²/s². $P(\Delta t)$ represents an integral of variability power for the region of time scale $\geq \Delta t$. It is easy to prove that $P(\Delta t_1) \geq P(\Delta t_2)$ if $\Delta t_2 > \Delta t_1$. Thus we can define the power density $p(\Delta t)$ in the time domain as the rate of change of $P(\Delta t)$ with respect to the time step Δt

$$p(\Delta t) = \frac{dP(\Delta t)}{d\Delta t}, \quad (6)$$

in counts²/s³ or rms²/s. With Eq. (5) and (6), we can calculate the power density spectrum in the time domain for a light curve. In practice, the differential calculus in Eq. (6) can be performed numerically

$$p(\Delta t) = \frac{P(\Delta t_1) - P(\Delta t_2)}{\Delta t_2 - \Delta t_1}, \quad (7)$$

with $P(\Delta t_1)$ and $P(\Delta t_2)$ being the two powers at the time scale Δt_1 and Δt_2 ($\Delta t_2 > \Delta t_1$), respectively, and $\Delta t = (\Delta t_1 + \Delta t_2)/2$.

To detect the source signal in a power spectrum against a noise background, we need to know the noise power $P_{noise}(\Delta t)$ of a time series consisting only of noise. For a white noise series where the $x(k)$ follows the Poisson distribution, the noise power is

$$P_{noise}(\Delta t) = \frac{\text{Var}(x)}{(\Delta t)^2} = \frac{\langle x \rangle}{(\Delta t)^2} = \frac{r}{\Delta t}, \quad (8)$$

where $\langle x \rangle$ is the expectation value of x , but with units of counts², which also the variance of the Poisson variable x , and r is the expectation value of the counting rate which can be estimated by the global average of counting rate of the studied observation. The noise power density at $\Delta t = (\Delta t_1 + \Delta t_2)/2$ is

$$p_{noise}(\Delta t) = \frac{P_{noise}(\Delta t_1) - P_{noise}(\Delta t_2)}{\Delta t_2 - \Delta t_1} = \frac{r}{\Delta t_1 \Delta t_2}. \quad (9)$$

The signal power density can be defined as

$$p_{signal}(\Delta t) = p(\Delta t) - p_{noise}(\Delta t) \quad (10)$$

and the fractional signal power density as

$$p'_{signal}(\Delta t) = \frac{p_{signal}(\Delta t)}{r^2}, \quad (11)$$

in units of 1/s or (rms/mean)²/s, where both 'rms' and 'mean' refer to the time series.

To study the signal power density in the time domain over a background of noise in an observed photon series, we divide the observation into M segments. For each segment

i , the signal power density $p_{i,signal}(\Delta t)$ is calculated by Eq. (10). The average power density of the studied observation is $\bar{p}_s = \sum_{i=1}^M p_{i,signal}/M$ and its standard deviation is $\sigma(\bar{p}_s) = \sqrt{\sum_{i=1}^M (p_{i,signal} - \bar{p}_s)^2 / (M(M-1))}$. We can use the statistical methods based on the normal distribution to make statistical inference, e.g. significance test, on \bar{p}_s . At short time steps, the number x of counts per bin may be too small for it to behave as a normally distributed variable. But it is easy to get a large enough total number (M) of segments from a certain observation period to satisfy the condition for applying the central limit theorem as well as for using the normal statistics on the mean \bar{p}_s .

To compare the power spectrum in the time domain with the Fourier spectrum for the same process, we study three different kinds of time series.

(1) *Periodic signal*

We use Eq.(5) and (6) to calculate the power density spectrum in the time domain for a sinusoidal process with a period of 0.5 s. In Figure 1, a piece of the counting rate curve of the studied process is shown in the top panel and the power density distribution of time scale of the sinusoidal signal is shown by the solid line in the middle panel. From the rate curve, we derive a corresponding counting series with a time step 2 ms and use 8192-point FFTs to get the Fourier power densities $p_f(f_j)$ and the corresponding densities in the time area $p_f(\Delta t_j = 1/f_j) = p_f(f_j)f_j^2$. The Fourier spectrum is shown by the dashed line in the middle panel of Fig. 1. The areas under the two power density curves in Fig. 1 are the same, as dictated by Parseval's theorem. It is obvious that the Fourier spectrum can not be interpreted as the distribution of variability amplitude vs. time scale. The power being concentrated at the sinusoid frequency f does not mean that the intensity variation of the process exists only at the corresponding time scale $1/f$. From the light curves with time steps $\Delta t = 0.05$ s and 0.28 s, shown in the bottom panel of Fig. 1, we can see that variation of the intensity definitely exists at time scales $\Delta t < 0.5$ s, but almost no power does in the Fourier spectrum at those time scales. In contrast with the Fourier spectrum, the power density spectrum determined in the time domain (the solid line in the middle panel of Fig.1) gives a proper description of the variability amplitude distribution of time scales.

Figure 2 shows the power density spectrum (the solid line in the bottom panel) derived in the time domain and the corresponding Fourier spectrum (the dashed line in the bottom panel) for a periodic triangular signal (the top panel). The Fourier spectrum is obtained with 8192-point FFT for a light curve with time step 1 ms. The many peaks at short time scales in the Fourier spectrum (high frequency harmonics) do not mean that there really exist strong variations in the process at those time scales, which are just necessitated by mathematically decomposing the triangular signal into sine waves. As a result, a Fourier spectrum may overestimate power densities at short time scales (high frequency harmonics

region) for a periodic signal with pulse shape being far from a sinusoid.

(2) *Stochastic Shots*

We now consider the power spectra of a signal $s(t)$ consisting of stochastic shots. Both the rise and decay fronts of the shots are an exponential with a time constant τ taken uniformly from the range between 5 ms and 0.2 s. The separation between two successive shots is exponentially distributed with an average separation $d = 0.5$ s. The average signal rate is assumed as $\bar{r}_s = 300$ cts/s. The peak height of the shot follows a uniform distribution between zero and the maximum. The top panel of Fig. 3 shows a piece of the signal counting curve with time step $\Delta t = 0.01$ s and the solid line in the bottom panel of Fig. 3 is the power density spectrum in the time domain expected for the signal $s(t)$. A simulated 2000 s light curve $x(k)$ with 1 ms time step is produced by a random sampling of the signal curve with Poisson fluctuations plus a white noise with mean rate 5000 cts/s. The middle panel of Fig. 3 shows a piece of the light curve with $\Delta t = 0.01$ s obtained from the simulated 1 ms light curve. In calculating the signal power density at a time scale Δt , The total light curve with time step Δt was divided into M data segments with $N = 100$ bins each. If the segments number $M < 100$ in cases of large time scales, we let $M = 100$ and decreased the number N of data points in each segment accordingly. For each segment of the light curve with time bin Δt_1 , the total powers at two time scales Δt_1 and $\Delta t_2 = 2\Delta t_1$ through Eq. (5) were calculated. The corresponding noise powers were calculated by Eq. (8) with r set equal to the average counting rate. The total power density $p(\Delta t)$ and noise power density $p_{noise}(\Delta t)$ at $\Delta t = 1.5\Delta t_1$ can be calculated by Eq. (7) and (9), respectively. Finally, the signal power density in the time domain is $p_{signal}(\Delta t) = p(\Delta t) - p_{noise}(\Delta t)$. In the bottom panel of Fig. 3, the plus signs mark the average signal power densities at different time scales. For the same light curve with 1 ms time binning, we also calculated the Leahy density $w(f_j) = 2|a_j|^2/a_0$ for each $T = 4.096$ s segment, where a_j is the Fourier amplitude at frequency $f_j = j/T$ determined from a 4096-point FFT. It is well known that the noise Leahy density $w_{noise} = 2$, so the signal Leahy density can be written as $w_{signal}(f_j) = w(f_j) - 2$ and the Fourier power density of the signal is expressed by $p_{F,signal}(f_j) = w_{signal}(f_j)a_0/T$ (Leahy et al 1983, van der Klis 1988). The dashed line in the bottom panel of Fig. 3 shows the average Fourier power density spectrum of the signal with respect to time scale $\Delta t_j = 1/f_j$. As the characteristic time τ of a shot is taken in the range between 5 ms and 0.2 s, there should exist considerable variability over this time scale range as represented by the power density spectrum in the time domain expected for the signal $s(t)$ (the solid line in the bottom panel of Fig. 3) and by that obtained from the simulated data including noise (pluses in the bottom panel of Fig. 3). Figure 4 represents the power spectra for another shot model with shorter characteristic time constant τ between 0.5 ms and 2 ms, average separation between two

successive shots 3 ms, average signal rate $\bar{r}_s = 500$ cts/s, and noise rate 5000 cts/s. From Fig. 3 and Fig. 4 we can see that for a random shot series the Fourier spectrum is more or less consistent with the power spectrum in the time domain at time scales greater than the characteristic time scale of the model, but significantly underestimates the power densities at shorter time scales.

(3) Markov process

The Markov process or autoregressive process of first order can describe the character of the variability for many physical processes. A Markov process can be expressed as the following stochastic time series

$$u(k) = a \cdot u(k-1) + \epsilon ,$$

where ϵ is a Gaussian random variable with zero mean and unit variance, and the relaxation time of the process is $\tau = -\Delta t / \log |a|$ with Δt being the time step. The observed light curve for the signal is

$$s(k) = c \cdot u(k) + r_s \Delta t ,$$

where r_s is the average rate of the signal. We make a light curve of the signal $s(k)$ with $\Delta t = 0.01$ s, $\tau = 0.1$ s, $r_s = 2000$ cts/s and $c = 2.5$. A piece of the produced signal light curve is shown in the top panel of Fig. 5. The final observed light curve $x(k) = s(k) + n(k)$ with $n(k)$ being a Poisson noise with mean rate 5000 cts/s, is shown in the middle panel of Fig. 5. In the bottom panel of Fig. 5, the solid line shows the power density distribution expected for the signal $s(k)$, the plus signs indicate excess power densities in the light curve $x(k)$ estimated by Eqs. (5)-(10) and the dashed line by FFT. From Fig. 5, we can see, similar to the case of stochastic shot process, that the proposed algorithm of evaluating power densities in the time domain is capable of extracting the power spectrum of the signal from noisy data and that the Fourier spectrum significantly underestimate the power densities at time scales around or shorter than the characteristic time scale of a stochastic process.

3. ACCRETING NEUTRON STARS AND BLACK HOLES

As revealed by above study based on simulations, the power density spectrum derived in the time domain can describe the real power distribution with respect to time scale for different time processes. The two kinds of power spectrum, Fourier spectrum and spectrum in the time domain, differ in ways depending on models of the processes. By comparing the two power spectra, more information about the nature of the variability of an object can be extracted. For this purpose we calculate both the power density spectra in the time domain

and Fourier spectra for the publicly available data of the Proportional Counter Array (PCA) aboard the Rossi X-ray Timing Explorer (RXTE) for a sample of X-ray binaries, 7 neutron stars and 7 black hole binaries. The PCA observations of X-ray objects included in our study are listed in Table 1. For each analyzed observation, we use the version 4.1 of standard RXTE ftools to extract the PCA data. At 18 time steps between 0.001 s and 2.5 s, we make the corresponding light curves with ~ 2000 s duration in an energy band as noted in Table 1. Then we remove all ineffective data points caused by failure due to the satellite, detector or data accumulation system, and calculate the power density spectra in the time domain, being based on a similar procedure in our simulation. The corresponding Fourier spectra are constructed by using 2^{-12} s ($\sim 244 \mu\text{s}$) time resolution light curves divided into parts containing 8192 bins.

Figure 6 shows the results from 6 observations for 5 neutron star binaries: KS 1731-260, 4U 1705-44, GS 1826-24, 4U 0614+091, 4U 1608-522 in the low state and 4U 1608-522 in the high state. The two kinds of power spectrum in the studied accreting neutron stars are generally consistent with each other, at least for the continuum dominated region. The feature is rather complicated for such sources whose Fourier spectra have significant quasi-periodic oscillation (QPO) structure. The left panel of Fig. 7 is from the QPO source, Sco X-1, whose power density spectrum in the time domain also shows a strong QPO structure but the peak shifts to shorter time scales due to the steep slope of the sinc function near the Nyquist frequencies (7 - 12.5 Hz) as more and more of the 6+ Hz QPO is accommodated by the time sampling. The difference between the spectrum of time domain and the Fourier spectrum at short time scales for Cyg X-2 (see the right panel of Fig. 7) may also be caused by QPOs.

For black hole candidates, we first analyze the canonical source Cygnus X-1. On May 10, 1996 (day 131 of 1996), the All-Sky Monitor on RXTE revealed that Cyg X-1 started a transition from the normal low (hard) state to a high (soft) state. After reaching the high state, it stayed there for about 2 months before going back down to the low state (Cui et al 1997). During this period, 11 pointing observations of Cyg X-1 were made by RXTE. We use one observation of PCA/RXTE for each of the four states of Cyg X-1. The signal power density spectra in the time domain of Cyg X-1 are shown by the plus signs in Fig. 8 and the corresponding Fourier spectra by the dots in Fig. 8. The power spectra of Cyg X-1 in different states (Fig. 8) have a common trait that the Fourier spectra are significantly lower than the corresponding power spectra of time domain in the time scale region of $\Delta t < 0.1$ s.

Besides Cyg X-1, the black hole candidates GRS1915+105, GRO J1655-40, GX 339-4, and XTE J1550-564 also demonstrate a significant excess in the power spectra in the time domain in comparison with the corresponding Fourier spectra at time scales shorter than

~ 0.1 s (see Figure 9). But the another analyzed black hole binary, GRS 1758-258, with QPO structures in its Fourier spectrum behaves differently (Fig. 10).

4. DISCUSSION

A Fourier power density spectrum presented in the time domain can not be interpreted as the real power density distribution of the physical process studied. In principal, the power densities in the time domain can be derived from a Fourier spectrum only when one knows every power density spectrum in the time domain for each sinusoidal function at all Fourier frequencies and adds them up with weight factors being the Fourier amplitudes. We propose here studying power spectra directly in the time domain. The definition of the power $P(\Delta t)$ (Eq. 5) is based just on the original meaning of rms variation and the power density spectrum $p(\Delta t)$ (Eq. 6) represents the distribution of the variability amplitude vs. time scale. The power density spectrum $p(\Delta t)$ in the time domain obtained from an observation depends only on the intrinsic nature of the signal process and the statistical property of the observed data, as does the Fourier power spectrum in the frequency domain. Our simulation studies show that the proposed algorithm, Eqs. (7), (9) and (10), is capable of extracting power densities of the signal from noisy data (comparing the expected signal spectra, the solid lines in the bottom panels of Figs. 3 and 5 and in Fig. 4, with the spectra calculated from the noisy data, plus signs in corresponding plots). These results indicate that the technique of spectral analysis in the time domain is a useful tool in timing and worth applying in temporal analysis for different sources. From Figs. (1) - (5) one can see that the difference of the Fourier spectrum with the spectrum in the time domain is dependent on the model of time series and sensitive to the characteristic time of a stochastic process. We can then use the difference between two kinds of spectrum to study the intrinsic nature of a studied process.

The power spectra shown in Figs. (8) and (9) for black hole candidates have a common character that the Fourier spectra are significantly lower than the corresponding time-based spectra in the time scale region of $\Delta t < 0.1$ s, which is similar to the simulation results for the stochastic shot model (Fig. 3) or the Markov process (Fig. 5). The existence of stochastic shots in X-ray light curves of Cyg X-1 has been noticed for a long time. With an improved searching and superposing algorithm and PCA/RXTE data of Cyg X-1 in different states, Feng, Li & Chen (1998) find that the average shot profiles can be described by exponentials with characteristic time scales $\sim 0.01 - 0.1$ s. Pottschmidt et al (1998) point out that an autoregressive process of first order with a relaxation time τ of about 0.1 s can reproduce approximately the variability of Cyg X-1. Thus, the characteristics of time

process in Cyg X-1 revealed from our power spectral analysis is consistent with that from modeling its light curves. The black hole candidates GRS 1915+105, GRO J1655-40, GX 339-4 and XTE J1550-564 also demonstrate characteristics similar to Cyg X-1, indicating that a stochastic process with a characteristic time ~ 0.1 s may be common in accreting black holes. While the absence of the broad-band noise above approximately 100 Hz in black hole candidates has been noticed before (Sunyaev & Revnivtsev 2000), our analysis shows that the apparent absence in Fourier spectra is caused by the existence of a stochastic process with characteristic time ~ 0.1 s and by the insensitivity of the Fourier technique to detecting rapid variability in a stochastic process.

At the same time, the two kinds of power spectrum are more or less consistent for accreting neutron stars with continuum dominated Fourier spectrum, as shown in Fig. 6. Our simulation results, Figs. (3) - (5), show that for a stochastic process the two kinds of spectrum can be consistent with each other at time scales greater than the characteristic time of the process. Assuming that a significant variability of an accreting neutron star comes from a stochastic process with very short characteristic time constant $\tau \ll 1$ ms can explain the consistence of the two kinds of power spectrum observed in neutron star systems. Sunyaev & Revnivtsev (2000) find that the power density spectra of accreting neutron stars with a weak magnetic field have significant broad noise component at the frequency 500-1000 Hz. They suggest that those X-ray transients which demonstrate significant noise in their X-ray flux at frequencies above ~ 500 Hz should be considered neutron stars. Most sources studied in this work (neutron star systems 4U 0614+091, 4U 1608-522, GS 1826-24, 4U 1705-44, KS 1731-260, Cyg X-2, and black hole candidates Cyg X-1, GX 339-4, GRS 1915+105, GRO J1655-40, XTE J1748-288, GRS 1758-258) are also studied by Sunyaev & Revnivtsev (2000) and our results support their claim under the condition that the spectra and noise in their statement are restricted within the Fourier framework. In contrast to the results from Sunyaev & Revnivtsev (2000), our results are based on inferring the characteristic time from the relation between two kinds of spectrum, no matter what the absolute magnitude of power spectrum is. The characteristic feature we find appears in all spectral states of the black hole candidate Cyg X-1 and the same is true with the neutron star binary 4U 1608-522.

The characteristic features in rapid variability for two different kinds of X-ray binary in our sample, which associate significant stochastic processes at the time scale ~ 0.1 s for black hole candidates and $\ll 1$ ms for neutron stars, are revealed only in continuum or broad noise. The QPO components behave in a more complicated fashion, but can be understood through the sensitivity of the time-based spectrum to variation at $2\delta t$, i.e., at half the Fourier sampling frequency (the Nyquist frequency). It has been found that QPO structures in power spectra can be caused by different kinds of signal, e.g., modulated

periodic signals and stochastic autoregressive processes with order ≥ 2 (van der Klis 1986). In the case of the neutron star binary Sco X-1 (the left plot of Fig. 7), the power density spectrum in the time domain reveals the QPO feature surprisingly well, though with a peak shifting to shorter time scales and with worse resolution.

Different processes with essentially different natures could result in almost the same Fourier power spectrum, thus distinguishing them is difficult through timing analysis only with the Fourier technique. This is a reason why we need to develop and apply alternative methods to supplement the Fourier technique in spectral analysis. Our results, though only preliminary, show that simultaneous use of both the Fourier and the time domain methods can help in probing the intrinsic nature of timing phenomena, and further, in distinguishing between different kinds of accreting compact object.

The authors thank the referee for helpful comments and suggestions and Dr. Qu Jinlu for help in data treatment. This work is supported by the Special Funds for Major State Basic Research Projects and the National Natural Science Foundation of China. The data analyzed in this work are obtained through the HEASARC online service provided by the NASA/GSFC.

REFERENCES

- Cui W., Zhang S.N., Focke W., & Swank J.H. 1997, ApJ, 484, 383
- Feng Y.X., Li T.P. & Chen L. 1999, ApJ, 514, 373
- Leahy D. A., Darbro W., Elsner R.F. et al., 1983, ApJ, 266, 160
- Li T. P., 2001, Chin. J. Astron. Astrophys., 1, 313
- Pottschmidt K., Konig M., Wilms J., & Staubert R. 1998, A&A, 334, 201
- Priestly M. B., 1981, Spectral Analysis and Time Series, London: Academic Press, 241
- Sunyaev R., & Revnivtsev M. 2000, A&AS, 358, 617
- van der Klis M., 1986, In: The physics of Accretion onto Compact Objects, ed by Mason K. O., Watson M. C., and White N. E., Lecture Notes in Physics, 266, 157
- van der Klis M., 1988, In: Ogelman E. P. J., van den Heuvel, eds., Timing Neutron Stars, Kluwer Academic Publishers, 27

Table 1. The used PCA observations of X-ray binaries

Type	Object	Observation	Band (keV)	Note
Neutron Star	KS 1731-260	10416-01-02-00	3-21	
	4U 1705-44	20073-04-01-00	3-20	
	GS 1826-24	30054-04-01-00	3-20	
	4U0614+091	30054-01-01-01	3-21	
	4U1608-522	30062-01-01-04	3-21	low state
	4U1608-522	30062-02-01-00	3-21	high state
	Sco X-1	30035-01-02-000	2-18	
	Cyg X-2	30418-01-01-00	2-21	
Black Hole	Cyg X-1	10412-01-01-00	2-13	low to high
	Cyg X-1	10512-01-08-00	2-13	high state
	Cyg X-1	10412-01-05-00	2-13	high to low
	Cyg X-1	10236-01-01-03	2-13	low state
	GRS1915+105	20402-01-05-00	5-22	
	GRO J1655-40	20402-02-25-00	5-22	
	GX 339-4	20181-01-01-00	4-22	
	XTE J1550-564	30191-01-14-00	2-13	
	GRS 1758-258	30149-01-01-00	3-21	
	XTE J1748-288	30185-01-01-00	2-21	

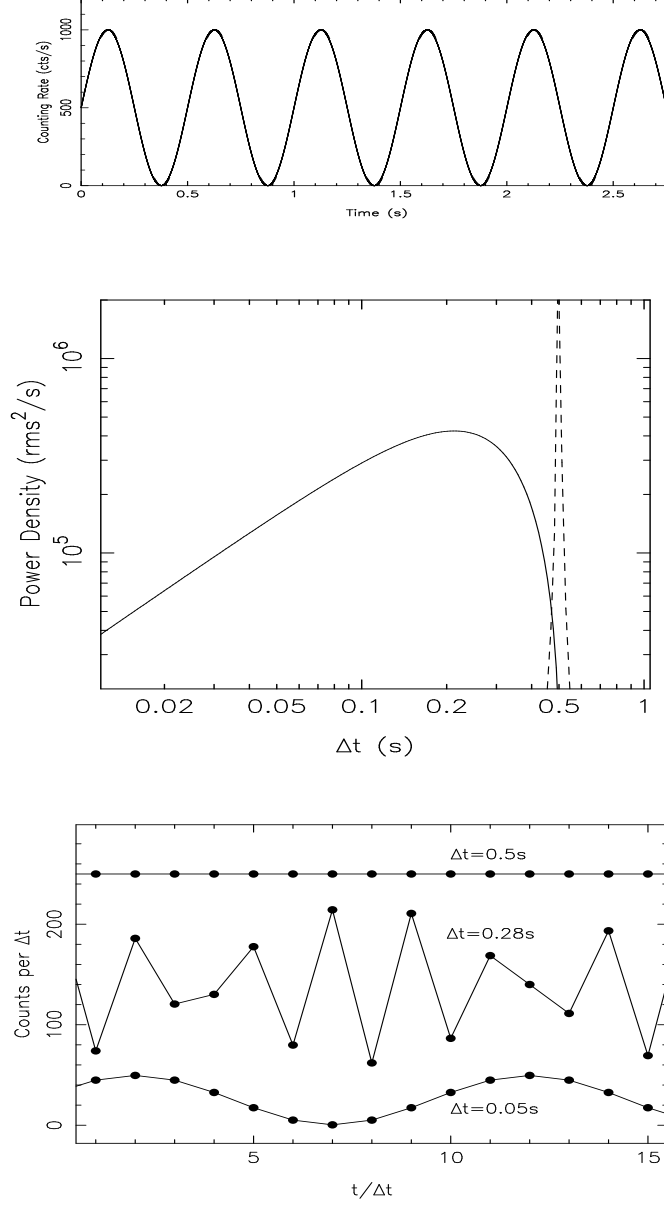


Fig. 1.— Distribution of power density vs. time scale of a sine signal. *Top panel:* counting rate curve of the sine signal with period 0.5 s. *Middle panel:* power densities. *Solid line* – power density spectrum derived in the time domain. *dashed line* – Fourier spectrum, derived by 8192-point FFT for the sine signal light curve with step 2 ms and shifted downwards by a factor of 100. *Bottom panel:* three light curves with time step 0.05 s, 0.28 s, and 0.5 s, respectively.

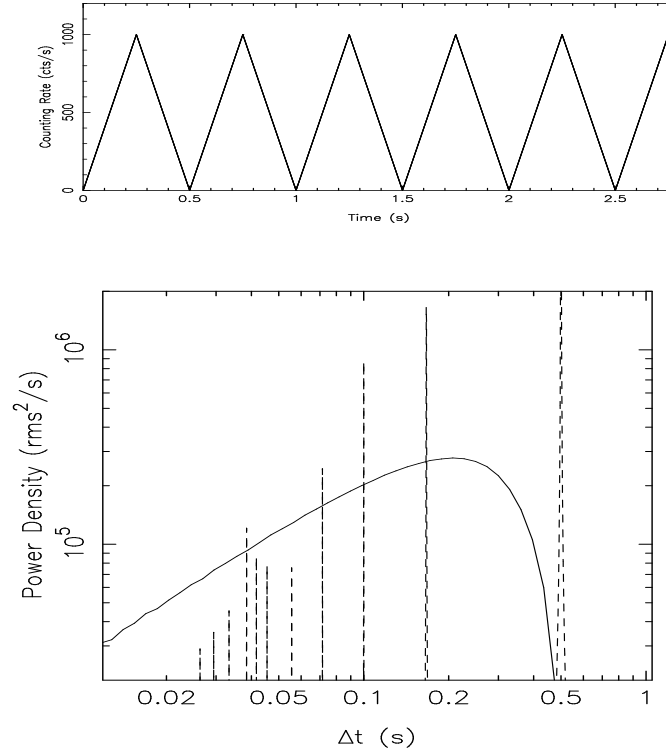


Fig. 2.— Distribution of power density vs. time scale of a periodic triangle signal. *Top panel:* counting rate curve of the periodic triangular signal with period 0.5 s. *Bottom panel:* power densities. *Solid line* – power density spectrum derived in the time domain. *dashed line* – Fourier spectrum, derived by 8192-point FFT for the the light curve of the signal with 1 ms step and shifted downwards by a factor of 80.

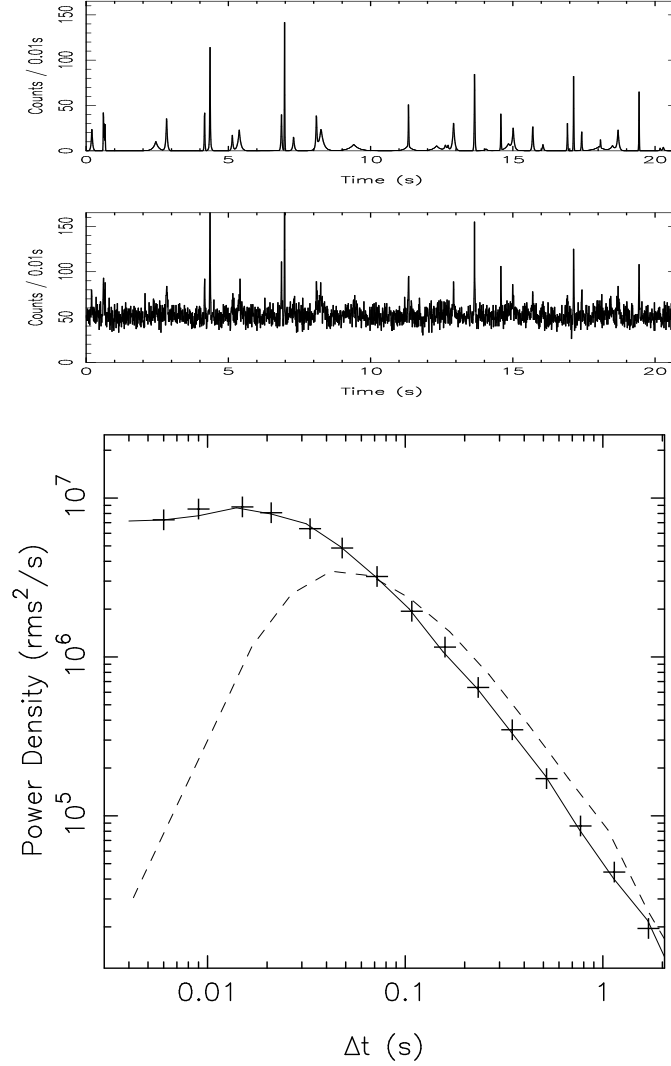


Fig. 3.— Distribution of power density vs. time scale of a shot model. *Top panel:* the signal, stochastic exponential shots with time constant τ between 5 ms and 0.2 s. *Middle panel:* simulated data which involved both signal and Poisson noises. *Bottom panel:* signal power densities. *Solid line* – power density distribution of time scale expected for the signal. *Dashed line* – excess Fourier spectrum from the simulated data. *Plus signs* – excess power densities calculated by the timing technique in the time domain for the simulated data.

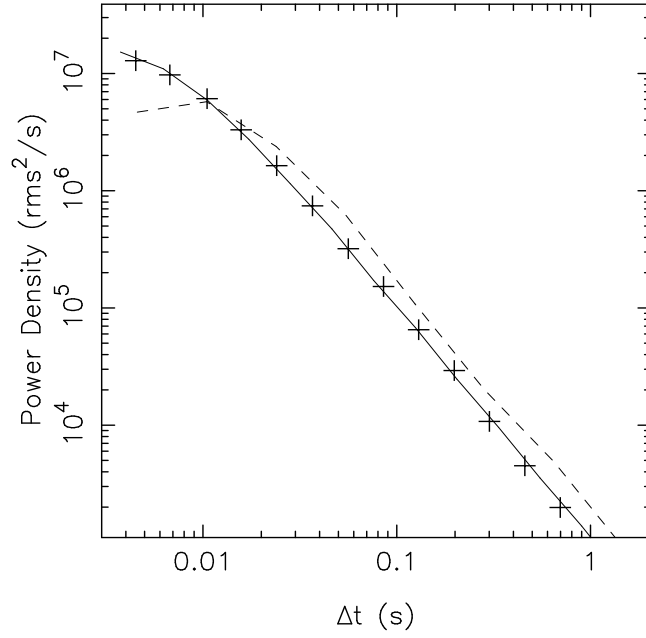


Fig. 4.— Distribution of power density vs. time scale of a shot model. Time constants of exponential shots are between 0.5 ms and 2 ms. *Solid line* – a theoretical distribution of power densities expected for the signal. *Dashed line* – the excess Fourier spectrum from the simulated data. *Plus* – the excess power densities calculated in the time domain for the simulated data.

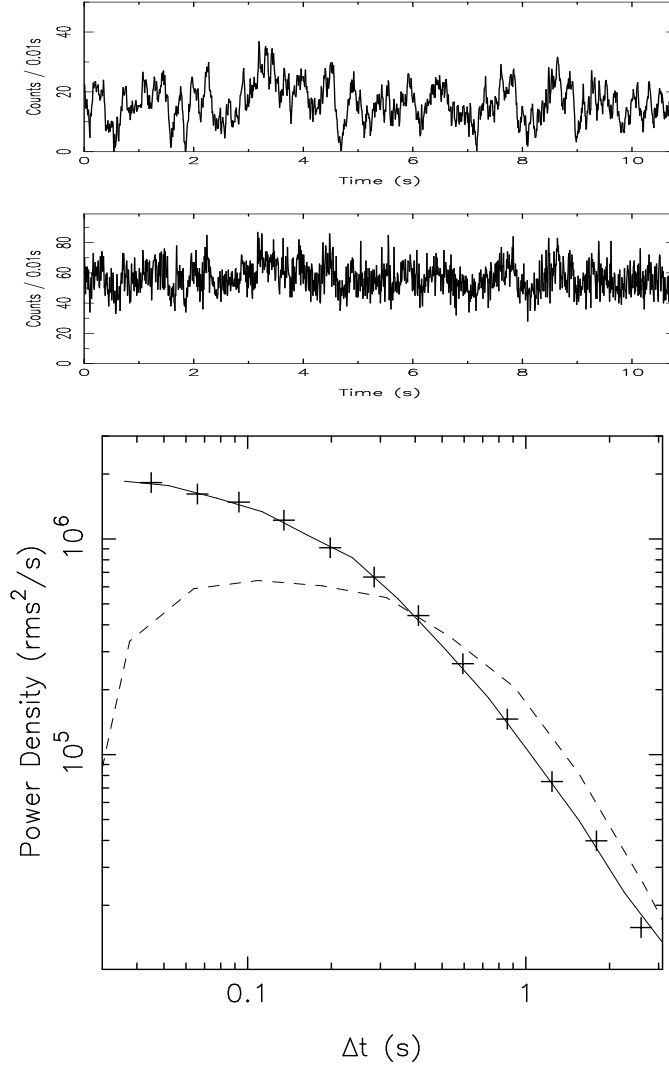


Fig. 5.— Distribution of power density vs. time scale of a Markov process. *Top panel:* the signal, a Markov process with relaxation time 0.1 s. *Middle panel:* simulated data which include signal and Poisson noises. *Bottom panel:* power densities of the signal. *Solid line* – the power distribution of time scale expected for the signal. *Dashed line* – excess Fourier spectrum from the simulated data. *Plus* – excess power densities calculated in the time domain for the simulated data.

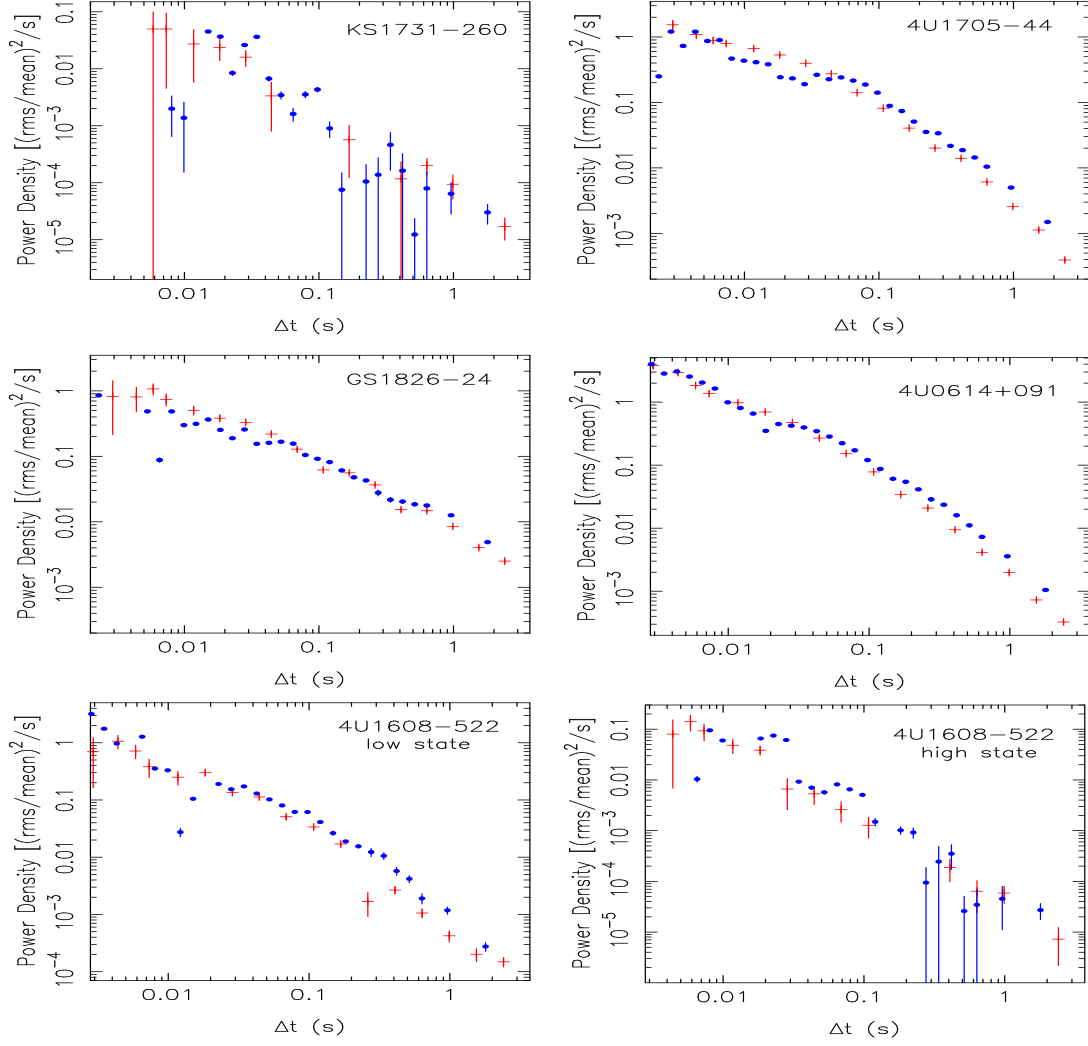


Fig. 6.— Power density vs. time scale of 5 accreting neutron stars. *Plus*: spectrum in the time domain. *Dot*: Fourier spectrum.

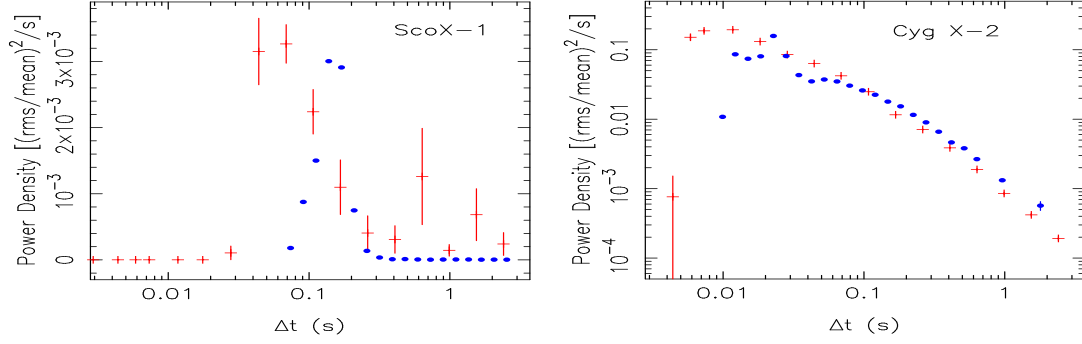


Fig. 7.— Power density vs. time scale of two accreting neutron stars. *Plus*: spectrum in the time domain. *Dot*: Fourier spectrum.

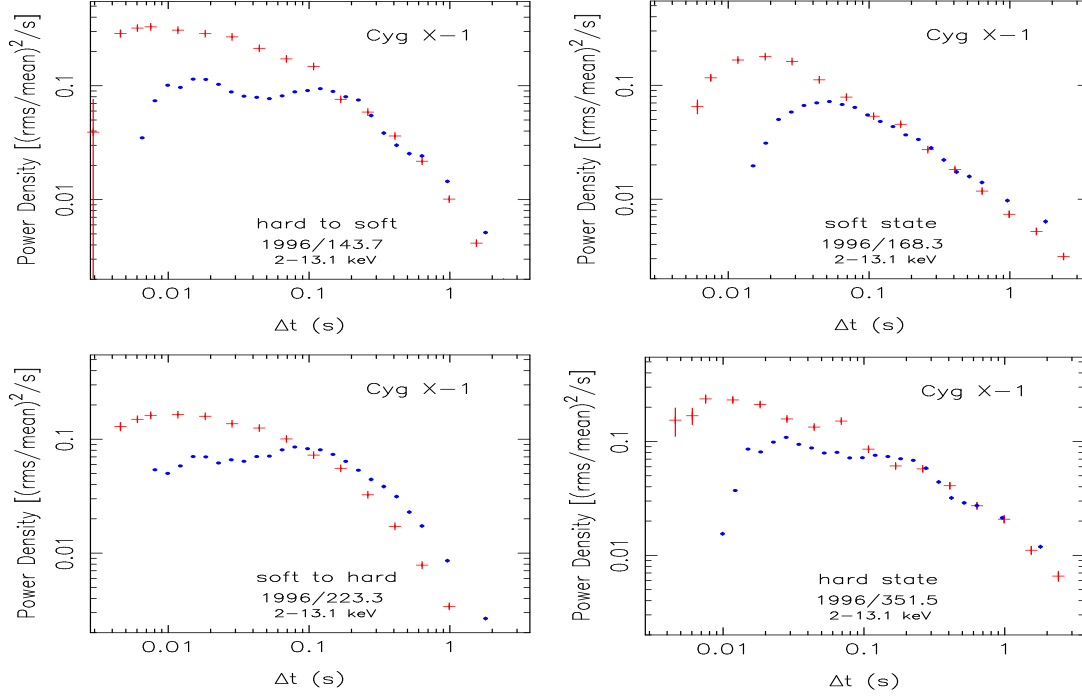


Fig. 8.— Power density vs. time scale of Cyg X-1. *Plus*: spectrum in the time domain. *Dot*: Fourier spectrum.

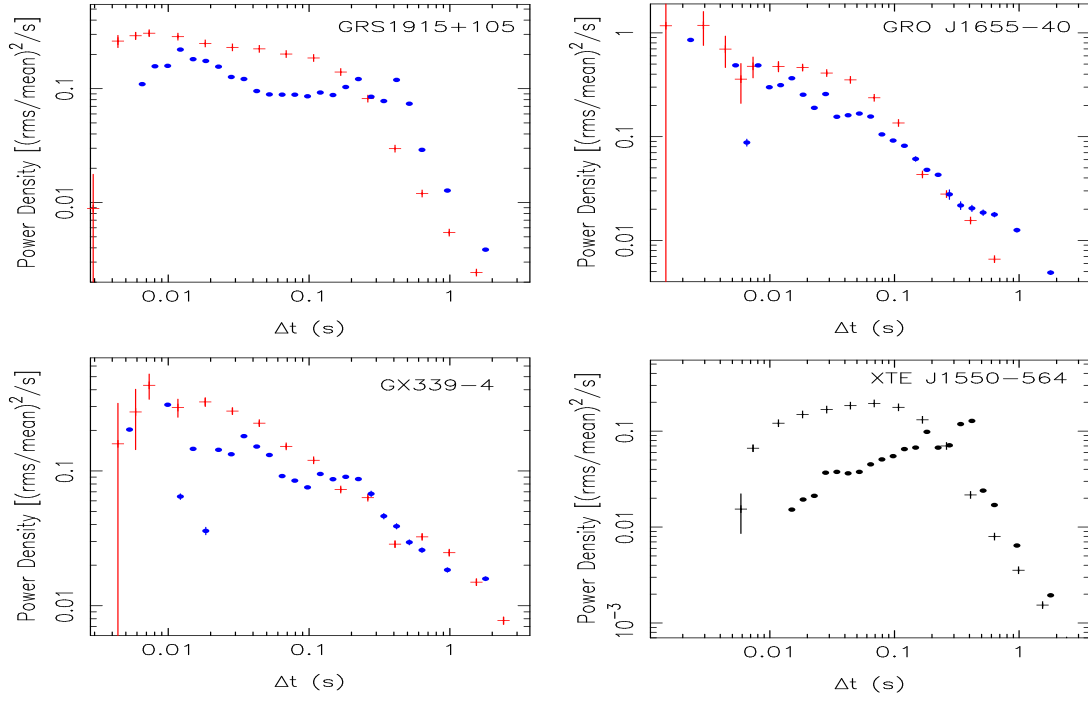


Fig. 9.— Power density vs. time scale of 4 accreting black holes. *Plus*: spectrum in the time domain. *Dot*: Fourier spectrum.

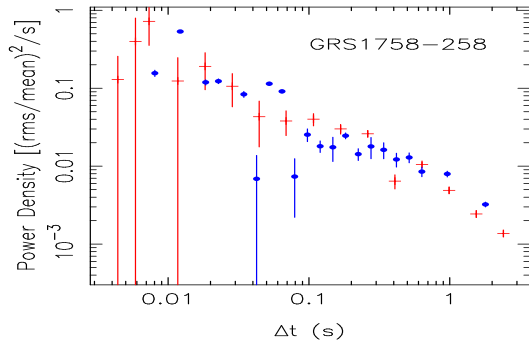


Fig. 10.— Power density vs. time scale of black hole binary GRS1758-258. *Plus*: spectrum in the time domain. *Dot*: Fourier spectrum.